

## Investigation of miniband formation in a graded-gap superlattice by electroreflectance spectroscopy

U. Behn

*Fachhochschule Schmalkalden, Blechhammer 4 und 9, D-98564 Schmalkalden, Germany*

N. Linder

*Institut für Technische Physik, Universität Erlangen-Nürnberg, Erwin-Rommel-Straße 1, D-91058 Erlangen, Germany*

H. T. Grahn and K. Ploog

*Paul-Drude-Institut für Festkörperelektronik, Hausvogteiplatz 5-7, D-10117 Berlin, Germany*

(Received 27 February 1995)

A graded-gap superlattice was investigated by electroreflectance (ER) at 80 K. With increasing electric-field strength the ER transitions of the individual wells exhibit first a redshift of 15 meV. At larger electric fields the typical blueshift of the Wannier-Stark localization is observed. This redshift of the transitions is explained by the formation of an electronic miniband at finite electric fields. This interpretation is supported by the calculation of the differential absorption as a function of the applied electric field. The calculations reproduce the main features of the experimental spectra.

In the past few years semiconductor superlattices have been the basis for many interesting optoelectronic and microelectronic applications, such as semiconductor lasers, optical modulators, or high speed transistors.<sup>1</sup> New electronic and optical properties arise when the coupling of electronic wave functions between adjacent wells occurs. In a conventional, strongly coupled superlattice, the electronic as well as the hole wave functions are delocalized at zero electric field, and minibands are formed in the conduction and valence bands.<sup>2</sup> When an electric field is applied parallel to the growth direction, first the hole minibands are destroyed. At the same time the electronic minibands split up into Wannier-Stark states, resulting in the well-known Wannier-Stark-ladder (WSL) transitions between valence and conduction band states with spatially indirect transitions.<sup>3,4</sup>

At even larger electric fields the electronic minibands are also destroyed, resulting in a complete localization of both the electronic and the hole states.<sup>3,4</sup> At very large electric-field strengths a delocalization of the electronic subbands between adjacent wells may occur, again due to the resonant coupling of different electronic subbands.<sup>5</sup> This is accompanied by an anticrossing of the participating optical transitions, resulting in a nonlinear optical behavior, which can be exploited for optical switches and modulators.<sup>6</sup>

Recently, the existence of a miniband at finite electric fields in a graded-gap superlattice was demonstrated by differential photocurrent spectroscopy (DPCS).<sup>7,8</sup> This superlattice consisted of 15 wells with an increasing energy gap of the well and barrier material. The experimental investigation showed a blueshift of about one-half of the miniband width in the DPC spectra, when the miniband was destroyed. However, the formation of the miniband at smaller electric fields could not be observed in the DPC spectra, because in this field range not all the wells contribute to the photocurrent.<sup>9</sup> Therefore, other optical methods, such as electroreflectance spectroscopy, which do not rely on carrier transport, are nec-

essary in this field range to investigate the formation of the miniband at finite electric fields.

In this paper we present clear evidence for the miniband formation in a graded-gap superlattice at finite electric fields as well as the destruction at larger electric fields. Electroreflectance (ER) spectroscopy is used in order to circumvent the problem of carrier transport. At the same time, this method is very sensitive due to its differential character. To clearly demonstrate the transition from localized to extended and back to localized states, the experimental results are compared to calculations of the differential absorption taking into account the complete sample structure.

The investigated sample consisted of 15 "periods" of 4.0 nm-2.0 nm  $\text{Al}_x\text{Ga}_{1-x}\text{As}-\text{Al}_y\text{Ga}_{1-y}\text{As}$  with a constant increase in the Al mole fraction from one period to the next. The superlattice was embedded in the intrinsic region of a *p-i-n* diode. The nominal Al mole fraction of the wells and barriers is given by  $x=0.03(n-1)$  and  $y=x+0.3$ , where  $n$  is the well number. Therefore, each quantum well has a different electron-hole transition energy. A total of 15 transitions with an average energy separation of about 25–30 meV is observed in the spectra. Further details on the sample structure are given in Ref. 8. The fit of the transitions in the DPC spectra<sup>7</sup> at large electric fields to the calculated energies showed that the actual sample parameters deviate from the nominal ones. The best fit of the transition energies was achieved with an Al mole fraction of 0.06 for the second well, followed by an increase between adjacent wells of  $\Delta x=0.015$  up to well 5, an increase of  $\Delta x=0.02$  between wells 5 and 7, and an increase of  $\Delta x=0.024$ , which is 80% of the nominal value for wells 7 to 15.

The ER spectra were measured in a standard configuration under normal incidence at 80 K. The modulation was performed using a square wave voltage of 50 mV with a frequency of 360 Hz. The electric field within the superlattice was varied by applying external dc voltages. In Fig. 1 a series of ER spectra taken at different dc voltages corre-

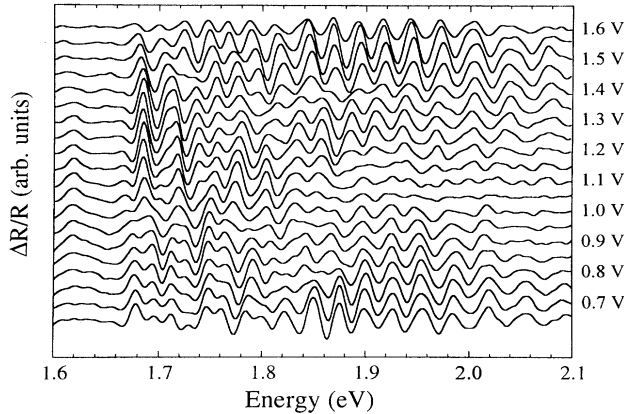


FIG. 1. Electroreflectance spectra of the graded-gap superlattice for different applied voltages between 1.65 and 0.65 V at 80 K. The spectra at different voltages have been shifted vertically for clarity.

sponding to different electric-field strengths is shown. The characteristic features as well as the flat-band voltage are shifted to larger voltages compared to the DPC spectra<sup>7</sup> because of the larger light intensity used in the ER measurements. In the energy range from 1.84 to 2.1 eV (subband transitions from well 7 to well 15) the ER transitions overlap in such a manner that every subband transition can be assigned to one ER oscillation as in the DPC spectra.<sup>7</sup> In the low energy region (between 1.6 and 1.84 eV) the ER line shape is more complicated, and an assignment of the transition energies is not possible for a variety of reasons. First, the coupling of the superlattice wells to the adjacent layers forming triangular wells causes a severe distortion of the first few superlattice energy levels at both ends. The calculations show that this effect is dominant in the low energy range of the spectra, leading to a series of resonances and anticrossings in the electric-field dependence of the transition energies. Second, the line shape of the ER spectra is in principle more complicated than the DPCS line shape. Although a first derivative excitonic line shape is expected for the investigated subband transitions,<sup>10</sup> it is not always straightforward to assign a distinct ER maximum or minimum exactly to a subband transition energy. Depending on the actual sample structure, in particular the number of overlayers and their thicknesses, the ER line shape is a sum of both the first derivative of the real and the imaginary part of the dielectric function. Furthermore, it can be influenced by interference effects within the superlattice itself.<sup>11–13</sup> Because of the large number of subband transitions and, consequently, the large number of free parameters, a line-shape fit of the ER spectra seems to be unreasonable. The oscillator strength of the light-hole transitions is about 30% of the heavy-hole transitions. Therefore, the light-hole transitions are neglected in the following.

A better overview of the electric-field dependence of the subband transitions is achieved in an isodensity plot of the spectra, which is shown in Fig. 2. In this figure the ER intensities are plotted as a function of the photon energy and applied voltage using a gray scale to indicate the strength of the ER intensity. We will from now on focus on transitions between the first heavy-hole and the first electronic subband

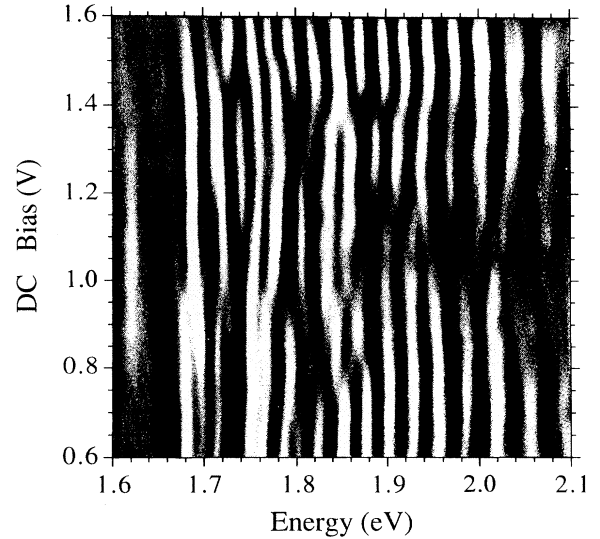


FIG. 2. Isointensity plot of the electroreflectance spectra at different applied voltages at 80 K. The darker areas correspond to minima in the electroreflectance signal.

( $H_{11}$ ) taking place in the center wells (7–12) of the superlattice, which corresponds to an energy range of 1.8–1.96 eV. We will distinguish three main electric-field regimes, as shown in Fig. 3. At small electric fields the states of the first electronic subbands are mostly localized within each well [regime I, see Fig. 3(a)]. For certain field strengths, the electronic subbands of all wells are resonantly aligned and form a miniband [regime III, see Fig. 3(b)]. At large electric fields the miniband is destroyed again, and the electronic states are localized in each well [regime V, see Fig. 3(c)]. The transition regions between I and III, i.e., regime II, and III and V,

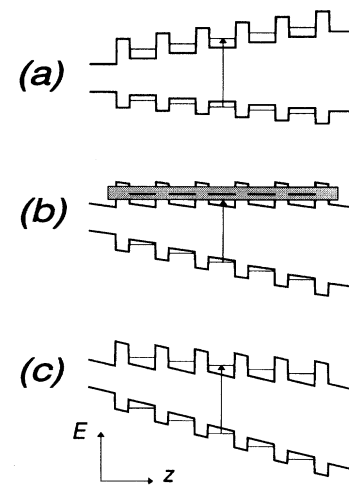


FIG. 3. Schematic conduction ( $\Gamma$ -edge) and valence band potential profiles in a compositionally graded superlattice for different values of the applied electric field: (a) flat band, (b) the field range corresponding to miniband formation in the conduction band, and (c) at large electric fields, when the conduction band states are completely localized again.

i.e., IV, correspond to the Wannier-Stark ladder regime. Starting from the miniband regime, each transition splits into several transitions with an energy separation of  $e\Delta V$ , where  $e$  is the electron charge and  $\Delta V$  the potential drop of the conduction band within one superlattice period. In regimes II and IV, the number of possible optical transitions increases significantly, and the oscillator strength of each individual quantum well transition is spread out over several WSL transitions. Therefore, a larger number of transitions is expected in regimes II and IV, and it will be difficult to spectrally resolve all of them.

At 1.6 V, which corresponds to a rather low electric-field strength, there are 15 oscillations visible, which obviously correspond to the subband transitions from the first heavy hole to the first electronic subband in each well. With decreasing applied voltage, i.e., increasing electric field, the transition energies remain nearly constant down to 1.45 V. This voltage range corresponds to regime I. The Stark shifts of all transitions can be neglected.<sup>7,9</sup> Between 1.45 and 1.35 V the transitions shift by about 17 meV to lower energies, and the oscillatory structure is less pronounced. This is the Wannier-Stark regime, i.e., the transition from localized to extended states (regime II). From 1.35 to 1.20 V the spectra change very little, showing again the transitions of each well. In this voltage range, the electronic states of each well are resonantly coupled, forming a miniband (regime III). Between 1.15 and 1.05 V the spectra show a very complex line shape with obviously many more than 15 transitions. The ER intensities are reduced due to the splitting of each subband transition into several Wannier-Stark transitions (regime IV). At 1.0 V the subband transitions reappear blueshifted by about 17 meV due to the complete Wannier-Stark localization of the miniband and remain constant in energy to larger electric fields (regime V). The blueshift as well as the redshift at smaller fields are expected to be about one-half of the miniband width. The deviations of the experimental spectra from the discussed features, in particular in the low and high energy parts of the spectra, are ascribed to the influence of boundary effects, the difference between the actual and nominal parameters, and the complex nature of the ER line shape.

In contrast to the previous work using DPCS, electroreflectance spectroscopy allows the investigation of not only the destruction of the electronic miniband at large electric fields, but also the formation of the miniband at small electric fields. To achieve further insight in the observed miniband formation at finite electric fields, we performed a simulation of the optical properties of the investigated sample. For that reason the superlattice potential as defined by the optimal fit parameters obtained above was embedded between two infinitely high confining potential layers. The absorption spectra were calculated from the set of wave functions and eigenvalues obtained by a numerical solution of the Schrödinger equation for electrons, heavy, and light holes. The validity of this approximation was tested by comparison with similar calculations, taking into account further layers of the real structure. The spectral features due to the central wells of the superlattice were unaffected by this procedure.

The results of the numerical calculations are shown in Fig. 4. Because of the large number of parameters used in the calculation, the comparison can only be qualitative. The cal-

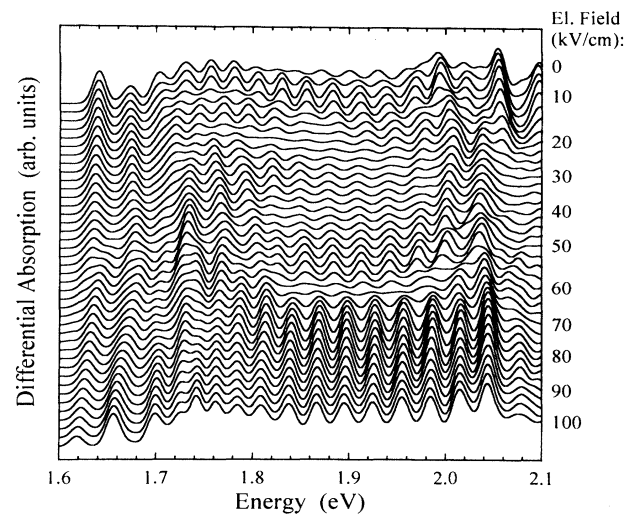


FIG. 4. Calculated differential absorption spectra of the graded-gap superlattice for different applied electric fields between 0 and 100 kV/cm. The spectra at different fields have been shifted vertically.

culated field dependence of the differential absorption coefficient clearly shows the five regimes discussed already in connection with the experimental results. Again the WSL regions, i.e., regimes II and IV, are confined to a rather small field range. The energy shift by about one-half of the peak distance is well reproduced for the redshift as well as the blueshift. It is, however, difficult to precisely predict the electric-field range in which the miniband exists. A voltage change between 1.4 and 1.05 V corresponds to a field change of about 25 kV/cm.<sup>8</sup> In the calculations the WSL regimes II and IV appear at electric-field strengths of 20 and 65 kV/cm, respectively. The difference between the calculated field strengths is twice as large as the experimental value. However, due to the regular potential profile used in the calculations, the estimated miniband width is still expected to be larger than that of the actual structure, shifting the WSL regions further apart. The calculated miniband width of about 45–60 meV agrees reasonably well with twice the observed shift of the optical transitions between complete localization and miniband regime.

In conclusion, we have investigated the miniband formation in a graded-gap semiconductor superlattice by electroreflectance. The formation of an electronic miniband at finite electric fields was unambiguously identified through a redshift of the corresponding optical quantum well transitions. The conventional blueshift due to the destruction of the miniband was also observed. Numerical simulations of the differential absorption of the investigated sample confirm the interpretation of the experimental spectra. The Wannier-Stark transition regimes at small and large electric fields are confined to a much narrower electric-field regime than in conventional superlattices.

We would like to thank A. Fischer for sample growth, F. Agulló-Rueda for stimulating discussions, and K.H. Schmidt and G.H. Döhler for experimental and theoretical support. This work was funded in part by the Bundesministerium für Forschung und Technologie.

- <sup>1</sup>See, e.g., C. Weisbuch and B. Vinter, *Quantum Semiconductor Structures* (Academic, Boston, 1991), Chap. 16.
- <sup>2</sup>L. Esaki and R. Tsu, *IBM J. Res. Dev.* **14**, 61 (1970).
- <sup>3</sup>E. E. Mendez, F. Agulló-Rueda, and J. M. Hong, *Phys. Rev. Lett.* **60**, 2426 (1988).
- <sup>4</sup>P. Voisin, J. Bleuse, C. Bouche, S. Gaillard, C. Alibert, and A. Regreny, *Phys. Rev. Lett.* **61**, 1639 (1988).
- <sup>5</sup>H. Schneider, H. T. Grahn, K. v. Klitzing, and K. Ploog, *Phys. Rev. Lett.* **65**, 2720 (1990).
- <sup>6</sup>See, e.g., F. Agulló-López, J. M. Cabrera, and F. Agulló-Rueda, *Electrooptics: Phenomena, Materials, and Applications* (Academic, New York, 1994).
- <sup>7</sup>F. Agulló-Rueda, A. D'Intino, K. H. Schmidt, G. H. Döhler, H. T. Grahn, and K. Ploog, *Europhys. Lett.* **23**, 283 (1993).
- <sup>8</sup>H. T. Grahn, F. Agulló-Rueda, A. D'Intino, K. H. Schmidt, G. H. Döhler, and K. Ploog, *Solid State Electron.* **37**, 835 (1994).
- <sup>9</sup>F. Agulló-Rueda, H. T. Grahn, A. Fischer, and K. Ploog, *Phys. Rev. B* **45**, 8818 (1992).
- <sup>10</sup>O. J. Glembocki and B. V. Shanabrook, *Superlattices Microstruct.* **5**, 603 (1989).
- <sup>11</sup>M. Nakayama, I. Tanaka, T. Doguchi, and H. Nishimura, *Jpn. J. Appl. Phys.* **29**, 1760 (1990).
- <sup>12</sup>A. J. Shields and P. C. Klipstein, *Phys. Rev. B* **43**, 9118 (1991).
- <sup>13</sup>U. Behn, H. T. Grahn, K. Ploog, and H. Schneider, *Phys. Rev. B* **48**, 11 827 (1993).

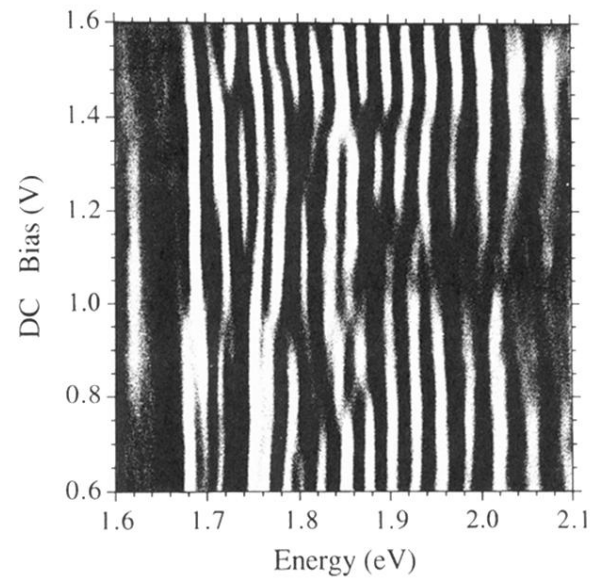


FIG. 2. Isointensity plot of the electroreflectance spectra at different applied voltages at 80 K. The darker areas correspond to minima in the electroreflectance signal.